Article

Energy Assessment of Second-Generation (2G) Bioethanol Production from Sweet Sorghum (*Sorghum bicolor* (L.) Moench) Bagasse

Iosvany López-Sandin [1,*], Rosa M. Rodríguez-Jasso [1], Guadalupe Gutiérrez-Soto [2], Gilver Rosero-Chasoy [1], Shiva [1], K. D. González-Gloria [1] and Héctor A. Ruiz [1,*]

1   Biorefinery Group, Food Research Department, School of Chemistry, Autonomous University of Coahuila, Saltillo 25280, Coahuila, Mexico
2   Facultad de Agronomía, Universidad Autónoma de Nuevo León, Francisco Villa S/N Col. Ex Hacienda El Canadá, General Escobedo 66415, Nuevo León, Mexico
*   Correspondence: losvany_fcq@uadec.edu.mx or iosvany.lopezs@uanl.edu.mx (I.L.-S.); hector_ruiz_leza@uadec.edu.mx (H.A.R.)

Abstract: Sweet sorghum bagasse (SSB) provides a raw material rich in polysaccharides that can be converted into biofuel and other high-value-added bioproducts under the biorefinery concept. The aim of this study was to evaluate the effect of hydrothermal pretreatment on the availability of SSB fermentable sugars for bioethanol production, considering the energy balance of the process. For this, the biomass was subjected to one process, pre-saccharification simultaneous and fermentation (PSSF). Previously, the temperature, time, and particle size effect were determined, as well as the enzymatic load for the more significant release of monomeric sugars. It was observed that the increase in the pretreatment severity, defined by the severity factor $[\log(R_o)]$, resulted in a more significant release of sugar and energy consumption. In the PSSF, bioethanol production was 22.17 g/L, with a total energy consumption of 2.46 MJ/g of processed biomass, of which 79.14% was by concept of electricity.

Keywords: biomass; energy integration; bioprocess; hydrothermal pretreatment; biorefinery; biofuels

1. Introduction

The continuous use of fossil fuels as the primary energy source has decreased their reserves and increased environmental pollution, intensifying the search for new renewable and environmentally friendly energy sources [1,2]. In this sense, biofuels produced from sustainable and renewable resources could be a potential alternative to meet the increase in energy demand [3,4]. Biomass-integrated biorefinery includes physicochemical processes for converting substrates rich in lignocellulose, triglycerides, sugar, and starch into biofuels [5,6], chemicals, and other bioproducts with the high added value that strengthens the production chain [7,8].

There is a wide variety of lignocellulosic materials rich in polysaccharides, such as agricultural crop residues. Between these can be mentioned sugar cane, sweet sorghum, and agave bagasse, in addition to rice, barley, and wheat straws [9]. Sweet sorghum bagasse (SSB) is an agro-industrial residue that has generated significant interest in biorefinery. It is mainly composed of cellulose, a potential source of fermentable sugars that can be transformed into biofuel [10]. Compared to other energy crops, sweet sorghum reduces the conflict between food and fuel [11]. Additionally, it is a fast-growing crop that adapts to various production conditions (climate, soil, stress tolerance, low input requirements, etc.) and produces high biomass volumes [12,13]. In biorefinery processes, pretreatment is a unitary operation that fractionates the biomass components and facilitates subsequent processes [2]. The selection of the pretreatment method, raw material, and the efficient use of biomass components (cellulose, hemicellulose, and lignin content) are determining

factors in the conversion and economy of the process [2,4]. Hydrothermal processing is a thermochemical pretreatment used to convert biomass into biofuels or high-value products, using water as a solvent and reagent under subcritical and supercritical conditions [14,15], characterized by its robustness, efficiency, and profitability [16]. Furthermore, it allows hemicellulose depolymerization (oligomers, monomers), lignin degradation (phenolic compounds), and the availability of cellulose increases [17]. Therefore, the pretreatment can be summarized as a set of actions that allow breaking the recalcitrant structure of the lignocellulosic biomass [18], among which are considered the supply of energy to increase the temperature and pressure of the system. These can be obtained by various energy sources whose effectiveness will be sufficient for operating parameters such as temperature, pressure, particle size, water-solid ratio, pH, gravity, and residence time [7,14,19].

In energy terms, biorefinery optimization focuses on the reduction in energy consumption. Thus, energy balances are decisive in understanding and comparing the various scenarios in which biorefinery processes are developed, establishing indexes for the quantification of energy flows in the systems based on the estimation and relationship between non-renewable energy required by the system and the energy produced by it [1,20]. The information obtained can be used to select the operating conditions that contribute to increasing energy efficiency [21]. In this sense, the biomass pretreatment selection, the method, and the technology to be used can represent an alternative that contributes to the recycling of nutrients, waste and energy reduction, and operating costs [3,22].

Therefore, this study aimed to evaluate the effect of hydrothermal pretreatment on the availability of SSB fermentable sugars for bioethanol production, considering the energy balance of the process. Figure S1 (Supplementary Materials) shows the block diagram of the process for obtaining bioethanol.

2. Materials and Methods

2.1. Raw Material

The SSB used in this study was obtained from the grinding of sweet sorghum cane [*Sorghum bicolor* (L.) Moench] harvested at the Marín Academic Unit, belonging to the School of Agronomy at the Autonomous University of Nuevo León (UANL) and was kindly provided to perform the corresponding pretreatment tests. To reduce the moisture content of the SSB and to be stored, it was placed in an oven (HAFO® 1600 series, USA) at 65 °C for 72 h.

2.2. Hydrothermal Pretreatment of Biomass (Autohydrolysis)

The SSB pretreatment process was carried out in the Biorefinery Laboratory. The moisture content of the SSB (7.62%) was determined in a thermobalance (AND® MF-50 Moisture Analyzer, Japan). These were reduced to 20 mm pieces and ground in a blade mill (PULVEX® Mini 100, Mexico) to decrease the particle size and increase the contact surface. Subsequently, the material was sieved and classified by size (0.5, 1.0, and 1.5 mm). Finally, it was characterized to determine the main biomass constituents and, thus, the hydrothermal pretreatment effect. In each test, 10 g of biomass was used and combined with distilled water in a solid/liquid ratio of 1:10 (*w/v*). The mixture was deposited in a reactor that operated according to the temperatures established in the experimental design (Section 2.2.1) and maintained for the specified residence time (Table 1). The pretreatment was carried out under an isothermal heating regime, without agitation, in a batch reactor pressurized by batches of stainless steel, with a total volume of 190 mL and a working volume of 130 mL (≈70% of the total), in addition to the control of temperature and pressure, which received the heat supply by means of electrical resistance and the cooling by a water jacket system. This reactor was designed by the Biorefinery group at the Autonomous University of Coahuila (www.biorefinerygroup.com, accessed on 16 November 2022), with a proportional-integral-derivative (PID) controller for temperature and suitable for subcritical processes (Figure S2, Supplementary Materials). Once the residence time was over, it was cooled, and the resulting suspension was filtered to separate the solid phase

from the liquid phase. The solid obtained was repeatedly washed with distilled water to remove hemicellulose residues and dried at 50 °C for 48 h in an oven (Quincy lab Inc® 30 GC Lab Oven, USA). A sample (1 mL aliquots) was taken from the liquid phase and centrifuged at $4500 \times g$ rpm (DLAB® D1008, China) to obtain the supernatant. Both phases were characterized.

The degree of biomass solubilization (expressed as wt% on dry biomass) in the pretreatment experiments was determined by the weight (W) difference before and after the experiment using the following equation [23]:

$$\% \, solubilization = \frac{W_{initial \, biomass} - W_{treated \, biomass}}{W_{initial \, biomass}} \times 100 \tag{1}$$

The chemical composition of the original biomass and the hydrothermally treated samples was determined by acid hydrolysis of the solids. The contents of the main polysaccharides and ash were estimated by the standard analytical procedures of the National Renewable Energy Laboratory (NREL/TP-510-42618; NREL/TP-510-42622) [24,25]. The solid recovered after acid hydrolysis was dried in the oven (under the conditions described above) and weighed to determine Klason lignin by gravimetric method. The content of monomeric sugars, acetic acid, and oligomers was determined by the HPLC method (see Section 2.5). To determine the effect of the experimental conditions on the results obtained, the severity factor was used, which provides a relationship between the temperature and the reaction time of the isothermal process according to the following equations [5,15]:

$$[\log(R_o)] = [R_o Heating] + [R_o Isothermal \, process] + [R_o Cooling] \tag{2}$$

$$[\log(R_o)] = \left[\int_0^{t_{max}} \frac{T(t) - 100}{\omega} \, dt \right] + \left[\int_{ctrl}^{ctrf} exp \left[\frac{T(t) - 100}{\omega} \right] dt \right] + \left[\int_{t_{max}}^0 \frac{T\prime^{(t)} - 100}{\omega} \, dt \right] \tag{3}$$

where [$\log R_o$] is the severity factor; t_{max} (min) is the time needed to reach the maximum autohydrolysis temperature; ctrl and ctrf (min) are the times required for the isothermal period; $T(t)$ and $T'(t)$ (°C) are the temperature profiles in heating and cooling, respectively; ω is an empirical parameter related to the activation energy with a value of 14.75. The severity factor [$\log(R_o)$] was calculated using numerical integration to obtain the area under the temperature vs. time curve.

2.2.1. Experiment Design

A Box–Behnken three-factor design was used to evaluate the effect of SSB hydrothermal pretreatment on overall sugar yields and energy intake (energy efficiency). The independent variables evaluated were temperature (X_1), residence time (X_2), and particle size (X_3). The response or dependent variables were the sugar yield released in the form of oligosaccharides and monosaccharides (g/L) and energy intake (MJ/g). The central point was evaluated with one repetition, which generated a total of 13 experiments (Table 1). The results were analyzed considering the degree of precision of the polynomial equation expressed by the determination coefficient (R^2). Statistical significance for the analysis of variance (ANOVA) was verified by an F test at the 95% level of significance. The results of the different conditions were compared using a Tukey test with a significance level of $p < 0.05$. A correlation analysis was performed to determine the independent variables' effect on the severity factor, and the latter on the dependent variables, in addition to the pH effect on cellulose concentration. The analysis was complemented with the construction of response and correlation surface diagrams. The statistical software MATLAB® version R2017 was used for the analysis of experimental data, the prediction of the model, and the construction of diagrams.

Table 1. Box–Behnken experimental design for the analysis of the SSB pretreatment process.

Run	Treatment	X_1 (°C)	X_2 (min)	X_3 (mm)
1	1	−1	−1	0
2	2	−1	1	0
3	3	1	−1	0
4	4	1	1	0
5	5	−1	0	−1
6	6	−1	0	1
7	7	1	0	−1
8	8	1	0	1
9	9	0	−1	−1
10	10	0	−1	1
11	11	0	1	−1
12	12	0	1	1
13 *	13	0	0	0

Factors	Symbol	Levels		
		−1	0	1
T (°C)	X_1	170	180	190
t (min)	X_2	10	30	50
S (mm)	X_3	0.5	1	1.5

* Central point. T = reaction temperature; t = residence or retention time; S = particle size.

2.2.2. Energy Efficiency of Hydrothermal Pretreatment

The energy efficiency (η_T) of the pretreatment was calculated using the following equation [26,27]:

$$\eta_T = \frac{TSR}{TEC} \tag{4}$$

where TSR is the total sugar recovery, which was considered the recovery of sugar from the liquid and solid phase of the pretreatment ($g_{sugars}/g_{biomass}$); TEC is the total energy consumption ($MJ/g_{biomasa}$), which considered the energy invested in electricity, human labor, and water (see equations in Section 2.6.1) in the milling and pretreatment of the biomass.

2.3. Enzymatic Hydrolysis (Saccharification)
Enzymes

The *Trichoderma reesei* enzyme cocktails of commercial Cellic CTec2 and Cellic HTec2 used in this study were kindly provided by Novozymes (USA). Cellic CTec2 is a complex enzyme cocktail consisting of β-glucosidases and hemicellulases, while Cellic HTec2 contains endoxylanases for enzyme hydrolysis of hemicellulose. The initial cellulase activity (118 FPU/mL) to Cellic CTec2 was determined according to the National Renewable Energy Laboratory (NREL/TP-510–42628) method [28].

In the enzymatic hydrolysis, the biomass obtained from the SSB pretreatment conditions was used, which allowed a higher sugar content. The tests were carried out in triplicate in 125 mL Erlenmeyer flasks with a working volume of 50 °C and a stirring speed of 150 rpm in an orbital shaker with temperature control (SHEL LAB®, Mexico), using a solid loading of 10% (*w/v*). A cellulase/hemicellulase ratio of 1:2 (*v/v*) and a cellulase loading rate of 10 and 15 FPU/g glucans were used [29]. Aparicio et al. [29] reported that the supplement of hemicellulases can improve the enzymatic process conversion, since a low quantity of xylan is in the pretreated solid (cellulose + lignin), the hemicellulases increases the accessibility of glucan removing the hemicellulose and xylooligosaccharides redeposited on the solid [30]. A variance analysis (ANOVA) was performed to determine minimally significant differences ($p < 0.05$) between cellulase loading rates and their effect on glucose concentration (g/L). During the hydrolysis process, samples (1 mL aliquots) were taken at 24, 48, 72, and 96 h and centrifuged at 4500× *g* rpm (DLAB® D1008, China)

to obtain the supernatant. The resulting supernatant was analyzed by HPLC (Section 2.5). The saccharification yield (conversion of glucan to glucose, %) was calculated using the following equation [31]:

$$Saccharification\ yield\ (\%) = \frac{(Glucose) + 1.053(Cellobiose)}{1.111(f)(Biomass)} * 100 \tag{5}$$

where (*Glucose*) is the residual glucose concentration (g/L); (*Cellobiose*) is the residual cellobiose concentration after glucan hydrolysis (g/L); 1.111 is the cellulose conversion factor; 1.053 is the cellobiose conversion factor; (*f*) is the fraction of glucan on a dry basis (*g/g*); (*Biomass*) is the concentration of dry biomass at the beginning of enzymatic hydrolysis.

2.4. Pre-Saccharification Simultaneous and Fermentation (PSSF)

2.4.1. Inoculum Preparation

Saccharomyces cerevisiae CA-11 yeast was acquired by the microbiological collection of the Biological Engineering Center of the University of Minho, Portugal. The yeast was cultivated in a 500 mL Erlenmeyer flask with 125 mL of medium composed of 50 g/L glucose, 10 g/L peptone, and yeast extract, which were incubated at 35 °C with a stirring speed of 150 rpm for 16 h in an orbital shaker with temperature control (SHEL LAB®, Mexico). The cell suspension was aseptically centrifuged (4 °C, 5600 rpm, 15 min) in a centrifuge (HERMLE® Z 326 K, Germany), and the solid was resuspended in 0.9% NaCl at a final concentration of 200 g/L of fresh yeast [29].

2.4.2. Saccharification and Fermentation

In the saccharification, a cellulase/hemicellulase ratio of 1:2 (*v/v*) and a cellulase loading of 15 FPU/g glucan were used, which was the condition with the highest glucose yield obtained in the enzymatic hydrolysis assay (Section 2.3). The assay was performed in a continuously stirred tank bioreactor (CSTBR) (*my-Control* for MiniBio Reactor, Applikon® Biotechnology, The Netherlands) of 500 mL with a working volume of 150 mL for 24 h at a temperature of 50 °C, pH of 4.8, and at 150 rpm under semi-anaerobic conditions. Saccharification kinetics was monitored for 24 h and samples of 1 mL were taken at 0, 12, and 24 h for glucose quantification. After that, the temperature was adjusted to 35 °C and they were inoculated with 8 g/L of *Saccharomyces cerevisiae* CA-11 of fresh yeast in NaCl suspension (0.9% *w/v*) to start the fermentation. Thus, aliquots of 1 mL were taken at 0, 2, 4, 6, 8, 10, 12, 24, 48, and 72 h for the quantification of glucose and bioethanol. The samples taken in saccharification and fermentation were centrifuged at 4500 rpm (DLAB® D1008, China) to obtain the supernatant. These were analyzed by the HPLC method (Section 2.5); meanwhile, the results were expressed as ethanol conversion yield (%) using the following equation [30]:

$$Cellulose\ conversion\ (\%) = \frac{[EtOH]_f - [EtOH]_0}{0.51[f \cdot (Biomass) \cdot 1.111]} \times 100 \tag{6}$$

where $[EtOH]_f$ is the ethanol concentration at the end of the fermentation (g/L) minus any ethanol produced from the enzyme and medium; $[EtOH]_0$ is the ethanol concentration at the beginning of the fermentation (g/L), which should be zero; 0.51 is the conversion factor for glucose to ethanol based on stoichiometric biochemistry of yeast; f is the cellulose fraction of dry biomass (g/g); (Biomass) is the dry biomass concentration at the beginning of the fermentation (g/L); 1.111 converts cellulose to equivalent glucose.

2.5. Analytical Procedures

The hydrolysates obtained from the pretreatment were filtered through a 0.45 μm nylon filter and analyzed by a High-Performance Liquid Chromatography (HPLC) system (Agilent Technologies® 1260 Infinity II, Germany) with refractive index for glucose, xylose, arabinose, acetic acid, and degradation compounds using calibration curves of these

reactive-grade compounds to determine their concentrations. A MetaCarb 87 H column (300 mm × 7.8 mm, Agilent) was used for the analysis. The column temperature was 60 °C and the mobile phase was 0.005 mol/L of sulfuric acid, using a flow rate of 0.7 mL/min.

2.6. Energy Balance

In the energy balance, the input energy and the energy output in the process used the methodology proposed by López-Sandin [1] and Mayer et al. [32], considering the energy equivalent of the inputs used and the power calorific value of the bioethanol obtained (Table 2). The consumption data was compiled from the energy consumed by the equipment, facilities, supplies, and labor used in each stage of the process (grinding, pretreatment, acid hydrolysis, enzymatic hydrolysis, fermentation).

Table 2. Energy equivalents.

Concept		Unit	Equivalent Energy (MJ/Unit)	Source
Human labor	Manual	h	1.96	[1]
	Mechanized		1.05	[1]
Sulphury acid		kg	0.702	[33]
Sodium hydroxide		kg	10.41	[34]
Other chemicals		kg	8.74	[34]
Enzymes		kg	6.32	[34]
Yeasts		kg	6.32	[34]
Water		kg	0.005	[35]
Electricity		kWh	11.93	[1]
			Calorific power	
Bioethanol		kg	2.69	[36]

2.6.1. Energy Input

Energy input (E_{inp}) in MJ was determined by the following equation:

$$E_{inp} = EC_G + EC_H + EC_A + EC_E + EC_F = \sum_{i=1}^{i=n} E_{ER} + E_{HL} + E_{CR} + E_{EO} \tag{7}$$

where EC_G is the energy consumed in grinding the SSB (MJ); EC_H is the energy consumed in the hydrothermal pretreatment (MJ); EC_A is the energy consumed in acid hydrolysis (MJ); EC_E is the energy consumed in enzymatic hydrolysis; EC_F is the energy consumed in the fermentation process; E_{ER} is the energy consumed in electricity (MJ); E_{HL} is the energy consumed by human work (MJ); E_{CR} is the energy consumed in chemical reagents (MJ); E_{EO} is the energy consumed by other inputs such as water, enzymes, and yeasts (MJ).

Electricity consumption considered the electrical devices directly used in the processes, as well as the associated equipment and installations. Consumption data was recorded by an electric meter (STEREN® CAJ-HER-432, DF, China) with a frequency of one hour and for equipment and/or installations used for limited periods of time; it was measured during the period of use. The energy consumed in electricity (E_{ER}) was determined using the following equation:

$$E_{ER} = \sum_{i=1}^{i=n} C_{ER} * Q_{ER} \tag{8}$$

where C_{ER} is the electricity consumption by the equipment or electrical installation (kWh); Q_{ER} is the energy equivalent of electricity (MJ/kWh) shown in Table 2.

Energy consumed in human labors (E_{HL}) was determined by the following equation:

$$E_{HL} = \sum_{i=1}^{i=n} T_{HL} * Q_{HL} \tag{9}$$

where T_{HL} is the work time of the operator (h); Q_{HL} is the energy equivalent of human work (MJ/h) shown in Table 2.

Energy consumed in chemical reagents (E_{CR}) was determined by the following equation:

$$E_{CR} = \sum_{i=1}^{i=n} R_{CR} * Q_{CR} \tag{10}$$

where R_{CR} is the chemical reactant (kg); Q_{CR} is the energy equivalent of the chemical reactant (MJ/kg) shown in Table 2.

The energy consumed in other supplies (E_{EO}) was determined by the following equation:

$$E_{EO} = \sum_{i=1}^{i=n} S_{EO} * Q_{EO} \tag{11}$$

where S_{EO} is the consumed supply (kg); Q_{EO} is the energy equivalent of the supplies (MJ/kg) shown in Table 2.

2.6.2. Energy Output

Renewable energy output (E_{out}) was determined using the following equation:

$$E_{out} = EtOH_W * HHV_{EtOH} \tag{12}$$

where $EtOH_W$ is the bioethanol weight (g); HHV_{EtOH} is the higher heating value of bioethanol (MJ/g) shown in Table 2.

3. Results and Discussion

3.1. Raw Material Composition

SSB carbohydrate content before hydrothermal pretreatment was $32.65 \pm 1.47\%$ cellulose (determined as glucan), $20.8 \pm 0.61\%$ hemicellulose ($15.63 \pm 0.01\%$ xylan, $4.14 \pm 0.09\%$ arabinosyl groups, and 1.03 ± 0.04 acetyl groups), $27.87 \pm 1.92\%$ of lignin, $4.17 \pm 0.66\%$ of ash, and $14.51 \pm 1.17\%$ of other components. In general, polysaccharide fractions make up more than half of the material, while lignin makes up about $\frac{1}{4}$ of the total dry biomass content. The composition of this material was like that reported in other SSB studies, with values ranging from 31.48 to 41.75% for cellulose, from 18.20 to 28.30% for hemicellulose, and from 7.40 to 29.10% for lignin [37–40]. However, the variations in the SSB composition may be associated, among other causes, as well with variety, location, degree of maturation of the crop, agricultural practices, agronomic and climatic conditions of the production areas, and the analytical procedure [37]. Thus, some studies have focused on selecting genotypes with lower lignin content and, therefore, less recalcitrant, allowing the production of economically efficient biofuels [41], since the high content of lignin can become a physical barrier to accessing cellulose and hemicellulose [37]. Therefore, hydrothermal pretreatment constitutes an alternative to increasing the biopolymers' bioavailability [15]. It is worth mentioning that lignin is the primary plant cell wall component responsible for biomass recalcitrance to industrial processing. Its recalcitrant chemical structure, like a non-linear aromatic polymer built with chemically diverse and poorly reactive linkages, with a variety of monomer units, reduces the ability of any single enzyme to recognize and degrade. Therefore, lignocellulosic feedstock uses will depend on its recalcitrance, directly relational with lignin, which protects cellulose and hemicellulose [42].

3.2. Effect of Hydrothermal Pretreatment (Autohydrolysis) on Raw Material Composition

The ANOVA results (Table S1, Supplementary Material) showed a statistically significant difference ($p < 0.05$) in the cellulose percentage (determined as glucan) because of the main factors. A significant effect was also observed for the interaction ($p < 0.05$) between temperature and particle size. Therefore, temperature, time, and particle size influenced the final percentage of cellulose to a lesser or greater extent.

Correlation analysis (Table S2, Supplementary Material) between experimental process variables showed a high positive correlation (r > 0.8 < 1) between temperature and pretreatment severity. This was evidenced by the exponential increase in severity with increasing temperature values. Likewise, a positive correlation was observed because of retention time, with a gradual increase in the severity of the pretreatment (r > 0.2 < 0.4). Regarding the particle size effect on the severity of the pretreatment, these had a weak negative correlation (r < 0 > −0.2), indicating a slight increase in severity with its decrease. Hence, the pretreatment severity expressed by the factor [$\log(R_o)$] was defined mainly by retention time and temperature effect, coinciding with reports from other studies [27,29,43]. However, it is crucial to consider that particle size can affect the ratio between the surface area and volume of the particle and, thus, the accessibility of enzymes and microorganisms during enzymatic hydrolysis and fermentation, respectively [13,18]. In this sense, it has been reported that through SSB use, high yields of bioethanol with a particle size between 0.5 to 2.5 mm have been obtained [44].

Cybulska and Thomsen [16] reported that the pretreatment effectiveness to produce highly digestible fibers depends principally on temperature and, to a lesser extent, on retention time. Likewise, the latter has not had a significant effect on the statistical modeling. However, this result could be a function of the temperature range and time used. Therefore, regardless of the incidence level of the main factors, it is important to consider the combined effect of these on the severity degree of the pretreatment and, thus, on the biomass composition. On the other hand, the chemical reactions and rearrangements that occur during pretreatment must be considered, since they are mainly regulated by the severity and the biomass's original characteristics [45]. Therefore, studying the effect of different combinations of temperature, time, and particle size can be the basis for optimizing pretreatment conditions and obtaining fibers that allow greater enzymatic digestibility [46]. In this sense, it has been reported that the optimal [$\log(R_o)$] to obtain the maximum digestibility of the fibers produced should be between 3 and 4.5 [16]. Similarly, high severity values can favor sugar degradation reactions and generate unwanted by-products such as acetic acid, furfural, and 5-hydroxymethylfurfural, which in later stages come to inhibit the growth of microorganisms and reduce bioethanol yields [16,43]. In this sense, the severity values obtained under the conditions generated by the combination of the factors studied are in the reported range (Table 3).

On the other hand, the pH of the liquid fraction showed a high negative correlation (r < −0.8 > −1.0) with the pretreatment severity, decreasing approximately from 4.17 in the most severe pretreatment (Tt-4: 190 °C, 50 min, 1.0 mm) to 3.75 in the less severe pretreatment (Tt-1: 170 °C, 10 min, 1.0 mm) (see Table S2 (Supplementary Materials)), behavior that has been reported previously [29,43]. This could be associated with the elevated temperature that causes water autoionization and the degradation of the acetyl groups present in the biomass [47], causing an increase in the concentration of hydrogen ions that significantly reduces the pH [16,29], in addition to the action of the degradation compounds produced (Table 4), mainly by the release of acetic acid due to the deacetylation of hemicellulose and the degradation of 5-hydroxymethylfurfural (HMF) to furfural [14,43]. Thereby, pH control during pretreatment is essential to reduce the pentoses degradation that results in the formation of byproducts that function as inhibitory agents during enzymatic hydrolysis and fermentation [14,16,43].

Table 3. Solid phase composition after hydrothermal processing.

	EC				GC			Component (Dry Weight: %, *w/w*) *		
Tt	T	t	S	P	[log(R$_o$)]	pH	HTR	Cellulose	Hemicellulose	Lignin
1	170	10	1	0.71	3.75	4.66	7.22	33.75 ± 0.79 FG **	9.38 ± 0.61 A	26.02 ± 0.20 F
2	170	50	1	0.71	4.07	3.96	7.66	36.63 ± 0.16 EF	9.32 ± 0.24 A	30.40 ± 2.20 BC
3	190	10	1	1.26	3.90	3.92	5.74	41.09 ± 0.77 CD	7.78 ± 0.09 CD	30.53 ± 1.20 BC
4	190	50	1	1.26	4.17	3.60	6.76	52.48 ± 1.49 A	5.03 ± 0.50 F	32.53 ± 0.76 A
5	170	30	0.50	0.71	4.01	3.75	6.98	37.85 ± 0.62 DE	8.29 ± 0.49 A	29.80 ± 1.62 CD
6	170	30	1.50	0.71	3.93	4.01	8.09	33.68 ± 1.51 G	8.82 ± 0.58 AB	28.20 ± 1.31 E
7	190	30	0.50	1.26	4.09	3.75	5.71	44.10 ± 1.27 BC	5.45 ± 0.40 F	30.73 ± 0.50 BC
8	190	30	1.50	1.26	4.02	3.86	7.57	45.24 ± 1.73 B	6.48 ± 0.37 EF	31.13 ± 2.91 ABC
9	180	10	0.50	0.89	3.85	4.43	7.07	38.75 ± 0.86 DE	9.21 ± 0.68 A	28.27 ± 1.29 DE
10	180	10	1.50	0.89	3.76	4.54	8.53	37.97 ± 0.80 DE	8.72 ± 0.60 ABC	30.21 ± 1.12 BC
11	180	50	0.50	0.89	4.13	3.72	7.73	40.39 ± 1.23 CD	7.27 ± 0.60 DE	31.66 ± 1.98 AB
12	180	50	1.50	0.89	4.11	3.77	8.16	37.91 ± 1.24 DE	7.09 ± 0.37 DE	30.73 ± 1.41 BC
13	180	30	1	0.89	4.01	3.80	7.43	39.86 ± 2.36 DE	7.83 ± 0.19 BCD	31.58 ± 1.50 AB

Tt = treatment; EC = established conditions; GC = generated conditions; T = reaction temperature (°C); t = residence or retention time (min); S = particle size (mm); P = pressure (MPa); [log(R$_o$)] = severity factor; HTR = heating rate (°C/min). * Data are mean values ± standard deviation of triplicate experiments. ** Different letters in the same column indicate statistically significant differences ($p < 0.05$).

Table 4. Liquid phase composition after hydrothermal processing.

Tt	Compounds (g/L) *							
	Glucose	Xylose	Arabinose	Acetic Acid	Levulinic Acid	HMF	Furfural	XOS
1	0.15 ± 0.00	0.29 ± 0.00	0.23 ± 0.01	0.41 ± 0.02	0.00 ± 0.00	0.00 ± 0.00	0.01 ± 0.00	0.01 ± 0.00
2	0.17 ± 0.00	0.37 ± 0.03	0.37 ± 0.00	0.91 ± 0.21	0.03 ± 0.01	0.04 ± 0.00	0.36 ± 0.19	0.04 ± 0.02
3	0.18 ± 0.00	0.47 ± 0.02	0.47 ± 0.02	1.02 ± 0.04	0.03 ± 0.00	0.05 ± 0.00	0.45 ± 0.04	0.05 ± 0.00
4	0.21 ± 0.00	1.55 ± 0.10	0.12 ± 0.00	3.13 ± 0.06	0.06 ± 0.00	0.24 ± 0.02	5.67 ± 0.29	0.23 ± 0.02
5	0.18 ± 0.00	0.31 ± 0.02	0.36 ± 0.00	1.07 ± 0.36	0.02 ± 0.00	0.03 ± 0.01	0.18 ± 0.08	0.03 ± 0.01
6	0.18 ± 0.00	0.30 ± 0.00	0.36 ± 0.02	0.54 ± 0.04	0.00 ± 0.00	0.01 ± 0.00	0.09 ± 0.00	0.02 ± 0.00
7	0.19 ± 0.00	1.51 ± 0.03	0.48 ± 0.08	1.39 ± 0.10	0.05 ± 0.01	0.30 ± 0.03	3.77 ± 0.19	0.28 ± 0.03
8	0.18 ± 0.00	0.83 ± 0.12	0.17 ± 0.00	0.64 ± 0.12	0.04 ± 0.02	0.08 ± 0.02	1.58 ± 0.31	0.08 ± 0.02
9	0.17 ± 0.00	0.29 ± 0.01	0.29 ± 0.03	0.44 ± 0.01	0.04 ± 0.02	0.02 ± 0.00	0.10 ± 0.04	0.02 ± 0.00
10	0.16 ± 0.00	0.29 ± 0.00	0.28 ± 0.00	0.38 ± 0.00	0.02 ± 0.00	0.01 ± 0.00	0.05 ± 0.00	0.02 ± 0.00
11	0.19 ± 0.00	1.59 ± 1.49	0.26 ± 0.02	0.65 ± 0.08	0.03 ± 0.00	0.06 ± 0.01	0.84 ± 0.01	0.06 ± 0.01
12	0.18 ± 0.00	0.71 ± 0.04	0.31 ± 0.02	0.91 ± 0.09	0.04 ± 0.00	0.09 ± 0.01	1.20 ± 0.11	0.09 ± 0.00
13	0.17 ± 0.00	0.38 ± 0.00	0.31 ± 0.00	0.56 ± 0.02	0.03 ± 0.00	0.03 ± 0.00	0.36 ± 0.01	0.03 ± 0.00

HMF = Hydroxymethylfurfural or 5-hydroxy-methylfurfuraldehyde; XOS = Xylooligosaccharides. * Data are mean values ± standard deviation of triplicate experiments.

3.2.1. Hydrothermal Pretreatment Influence on the Solid Phase

The chemical composition of the SSB solid phase fibers with respect to the three main components of lignocellulose (cellulose, hemicellulose, and lignin) after hydrothermal pretreatment is shown in Table 3. The three-dimensional mathematical model to estimate the cellulose content (% of the total dry weight) and build the response surface graphs (Figure 1) showed that the experimental data had a high degree of fit (regression coefficient: $R^2 = 0.93$) with respect to the experimental design, using the following equation:

$$Celulose\ (\%) = 39.86 + 5.25T + 1.98t - 0.91S + 1.17T^2 - 0.04t^2 - 1.06S^2 + 2.13(T \cdot t) + 1.58(T \cdot S) - 0.43(t \cdot S) \quad (13)$$

where T is the pretreatment temperature (°C), t is the retention time (min), and S is the particle size (mm).
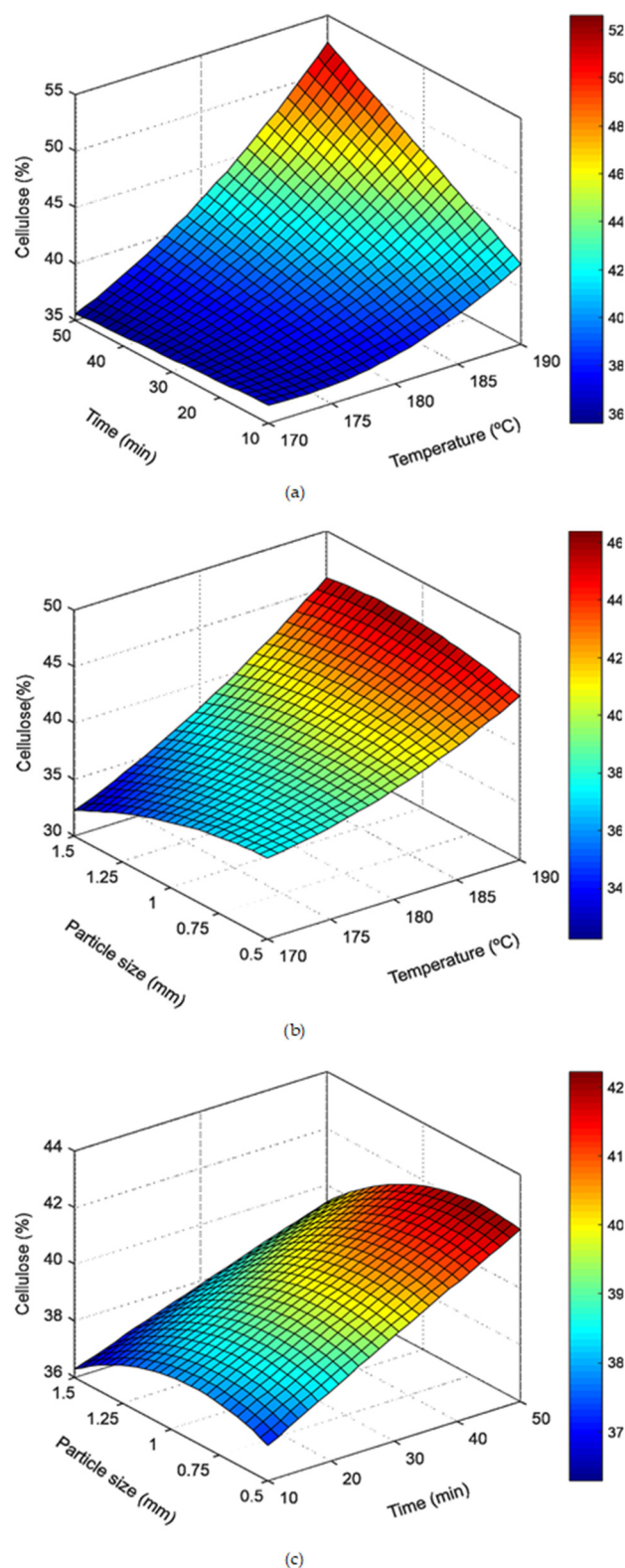
Figure 1. Cellulose response surface graphs (determined as glucan in % of total dry weight) under the operating conditions of the autohydrolysis pretreatment. (**a**) Temperature and time effect on cellulose concentration; (**b**) temperature and particle size effect on cellulose concentration; (**c**) time and particle size effect on cellulose concentration.

The higher percentage of cellulose (determined as glucan) and lignin (determined as soluble and insoluble lignin in acid) was obtained under the treatment conditions of

the higher [log(R_o)], coinciding with that reported in other studies [29,43]. Compared to untreated biomass, pretreatment at temperatures of 170, 180, and 190 °C increased cellulose availability by 6.98, 16.17, and 28.03%, respectively. Likewise, the lignin percentage increased from 27.87 to 32.53% with the most severe pretreatment (Tt-4), which can be explained by the changes that the chemical structure undergoes due to fusion, coagulation, and repolymerization with the fibers of cellulose [14]. This causes losses in carbohydrate concentration due to solubilization with an apparent increase in the lignin fraction resulting from the increase in acid-insoluble residues [14,16,46]. Similarly, the hemicellulose content (measured as xylan, arabinan, and acetic acid) showed a decrease with increasing treatment severity. This behavior was like what was previously reported in other investigations [15,23,43] and can be attributed to the fact that these compounds are hydrolyzed to the liquid phase, reaching their total solubilization with temperatures above 190 °C [14,43]. In this sense, the hemicellulose content with respect to the original biomass decreased from 53.97 to 75.07% with temperatures of 170 and 190 °C in the treatments of lesser (Tt-1) and greater (Tt-4) severity, respectively. In general, the pretreatment allowed the dissolution of a solid biomass fraction, whose yield depended on the severity degree of the experiment. Thus, the solubilization of the biomass increased with increasing values of [log(R_o)] and the reduction in the pH in the liquid, varying approximately between 2.8% (3 wt%) and 20.5% (20.5 wt%) in weight in the treatment of lesser (Tt-1) and greater severity (Tt-4), respectively (Figure 2). Nitsos et al. [23] reported similar behavior using different lignocellulosic biomasses, while Lin et al. [48] observed it in algae biomass. Finally, the most severe operating condition (Tt-4) was selected to be scaled and continued with the following enzymatic hydrolysis process, considering the response of the percentage of cellulose to the temperature effect, time, and particle size. Based on these results, in future research, the operating conditions of the process will be optimized to obtain a higher yield of sugar with a lower energy cost.
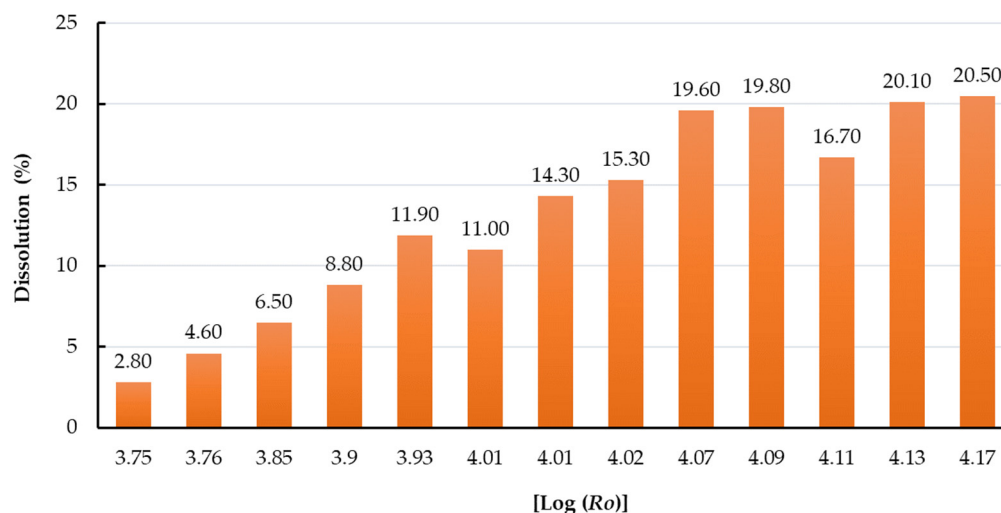
Figure 2. Effect of the severity of the pretreatment [log(R_o)] on the percentage of biomass dissolution.

3.2.2. Hydrothermal Pretreatment Influence on the Liquid Phase

Table 4 shows the chemical composition of the main hydrolysate compounds obtained during the hydrothermal pretreatment. In general, monomeric xylose was the majority sugar detected in the liquid, while glucose and arabinose were detected in a smaller proportion, according to what was reported for the SSB [49]. The sugars' concentration (including xylooligosaccharides) and carboxylic acids obtained in hydrothermal pretreatments can be explained by the high rate of degradation of hemicellulose [23], whose concentrations can vary depending on the severity [27,43]. Xylooligosaccharides (XOS) are sugar oligomers made with xylose units. They are recognized for their great prebiotic potential and nutritional benefits, promoting the growth of probiotic bacteria in the intestinal tract. Other

benefits of XOS are stimulating intestinal microflora, including lowering blood cholesterol and glycemic indices. Furthermore these reduce pro-cancer enzymes in the gastrointestinal tract, improve the absorption of minerals in the large intestine, and stimulate the immune system [50]. In addition, some XOS can promote root development as a plant regulator, a sugar supplement for people, and prebiotics to promote intestinal motility utilization health, increasing the added value of the process [51]. Thus, the hydrothermal pretreatment allowed the breaking of the recalcitrant structure of the biomass and obtaining a mixture rich in carbon that derives from the degradation of lignin, hemicellulose, small fractions of cellulose, and some inert components [13]. Therefore, the characterization of the liquid phase is necessary to know the concentration of unwanted components that inhibit enzymatic action [14,29], as well as the XOS bioactivity assay that can increase value-added products.

The Tt-11 treatment (180 °C, 50 min, 0.5 mm, $[\log(R_o)] = 4.13$) showed the higher xylose concentration (1.59 g/L), while Tt-4 (190 °C, 50 min, 1 mm, $[\log(R_o)] = 4.17$) had the higher glucose concentration (0.21 g/L). Regarding the concentration of arabinose, Tt-7 (190 °C, 30 min, 0.5 mm, $[\log(R_o)] = 4.09$) showed a higher concentration, demonstrating that the high-severity treatments had a greater sugar release. Regarding the degradation compounds of the hydrolyzate, carboxylic acids (acetic acid, levulinic acid), aldehydes (Furfural), and furans (hydroxymethylfurfural or 5-hydroxy-methylfurfuraldehyde, HMF) were detected. The treatments generally showed a higher concentration of furfural (5.67 g/L), followed by acetic acid (3.13 g/L), while the rest of the components were detected in lower quantities. Although these are unwanted compounds during the transformation of biomass to bioethanol, they can be used as raw material in the production of other value-added products [52] with potential applications in different areas (energy, food, materials, etc.), strengthening the biorefinery concept in terms of a circular bioeconomy [53,54].

3.2.3. Energy Efficiency of Hydrothermal Pretreatment

The energy balance for the different operating conditions of the SSB pretreatment is shown in Figure 3. Treatments Tt-1 (170 °C, 10 min, 1.0 mm; $[\log(R_o)] = 3.75$) and Tt-4 (190 °C, 50 min, 1.0 mm; $[\log(R_o)] = 4.17$) showed the lowest (0.160 MJ/g) and highest (0.320 MJ/g) energy consumption, respectively (Figure 3a), while treatment Tt-7 (190 °C, 30 min, 0.5 mm, $[\log(R_o)] = 4.09$) had the highest η_T value (1.22 g_{sugars}/MJ; Figure 4b). In this sense, the energy consumed can be explained by the positive correlation observed with the factor's temperature and retention time and, hence, with the $[\log(R_o)]$ (Table S2, Supplementary Materials). Thus, high energy efficiency can be achieved from the optimization of these parameters, in addition to the recovery of heat lost during pretreatment and the reduction in water use [48]. Shiva et al. [27] point out that energy efficiency can be affected by the volume of processed biomass and by the solid's load (>15% *w/v*). However, the above is not synonymous with reaching the maximum sugar yield, since high energy efficiency can be achieved [26,48], but with low sugar yields [26]. Thus, the highest η_T was related to obtaining a high concentration of sugar and reduced energy expenditure, as was observed in Tt-7. Although this treatment was not the one with the lowest energy consumption and highest sugar yield (Table 3), it did show the highest numerical value of η_T. On the other hand, the particle size did not have a direct effect on the energy consumption of the pretreatment (Table S2, Supplementary Materials). This can be explained by the difference in the size range used (0.5 mm), since the determining influence of particle size on the pretreatment energy efficiency has been reported [26]. Likewise, an alternative to improve energy efficiency is the combination of enzymatic pretreatment and hydrothermal treatment [27,36]. It is worth mentioning that the energy balance may depend on factors such as the origin, type, and chemical composition of the raw material, as well as the technology used in each process. In general, these results should be used to optimize the energy consumption of the pretreatment and achieve energy integration in the second-generation biorefinery, in addition to contributing to the generation of information that enriches future studies of energy balances.

(a)

(b)
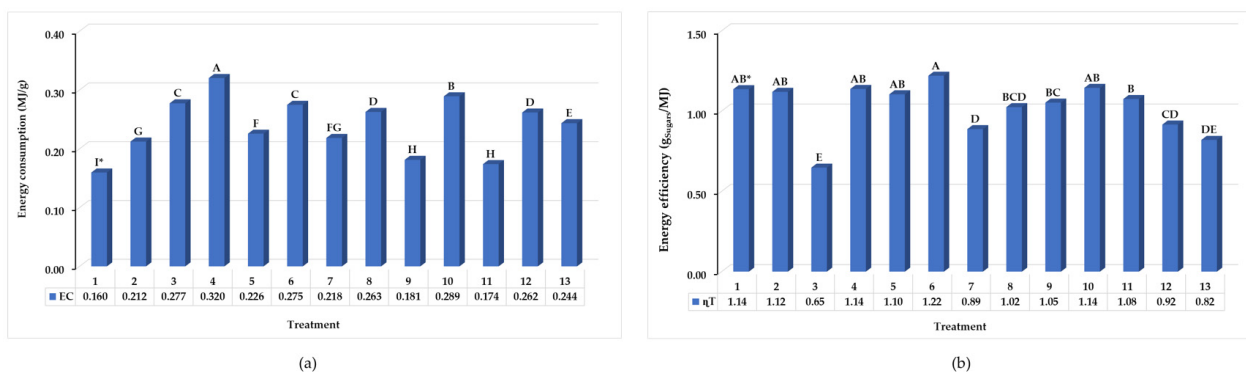
Figure 3. Energy balance in hydrothermal pretreatment. (**a**) Energy consumption (EC) per treatment; (**b**) energy efficiency (η_T) per treatment. * Different letters between bars indicate statistically significant differences ($p < 0.05$).

3.3. Enzymatic Hydrolysis

The enzymatic hydrolysis results showed that the release of sugars did not have statistically significant differences ($p > 0.05$) because of the independent variables evaluated. However, interaction ($p < 0.05$) was observed between them (Table S3, Supplementary Materials). The enzyme blends allowed the cellulose degradation to simple fermentable sugars with greater susceptibility to enzymatic action in the biomass pretreated. Meanwhile, the increase in the pretreated material digestibility can be explained by the modification of the lignin layer and the structural morphology, the increase in the surface area and porosity, and the decrease in the cellulose crystallinity [13,14,46]. Regarding the stability of the enzymatic activity, the treatments conserved most of it up to 72 h, tending to a linear behavior that later reaches equilibrium, showing the typical curve of enzyme kinetics [37,43]. Thus, the higher yield of monomeric sugars was observed at 24 h, with values of 79.06 and 71.25% for glucose, 80.41 and 75.96% for xylose, 45.08 and 52.84% for cellobiose, with loads of 10 and 15 FPU/g, respectively (Figure 4). Therefore, the hydrolysis process can be adjusted to 24 h using the lowest enzyme load, allowing the generated material to be used in a saccharification and fermentation process simultaneously [16]. In this sense, Thanapimmetha et al. [39] reported that enzyme load is a crucial factor in the rate and hydrolysis degree of a pretreated lignocellulosic substrate. Therefore, it must be optimized to reduce time and its impact on the economy of the process.

On the other hand, the saccharification process showed the classic kinetics of lignocellulosic biomasses [27,37,39,43]. The final concentration of monomeric sugars at 96 h of saccharification was 99.02 and 102.35 g/L for glucose (Figure 4a), 11.18 and 11.98 g/L for xylose (Figure 4b), and 5.28 and 5.81 g/L for cellobiose (Figure 4c), for a yeast load of 10 and 15 FPU/g, respectively. Compared to the control, the glucose, xylose, and cellobiose concentration of the enzymatic treatments had increases of 6.5, 1.7, and 11 times, respectively. Furthermore, they were higher than those reported for other sorghum varieties [37,39] and other lignocellulosic materials [27].

Moreover, the glucose concentrations observed in the treatments with 10 and 15 FPU/g were 80.08 and 82.63%, respectively (Figure 4d). It is worth mentioning that, in the first 24 h, the higher glucose release rate was observed at 2.93 and 3.04 g/L/h, respectively, which gradually decreased over time. In this sense, it has been reported that an increase in the concentration of monomeric sugars is associated with an increase in the solids load. However, the high viscosity of the substrate contributes to keeping the sugar concentration constant since it limits mass transfer and the possible inhibition of cellulases due to the high content of glucose and cellobiose [37,43]. In addition, the effect of enzyme blend used to catalyze the cellulose decomposition into simple sugars may vary due to the characteristics of the biomass and the pretreatment [14].
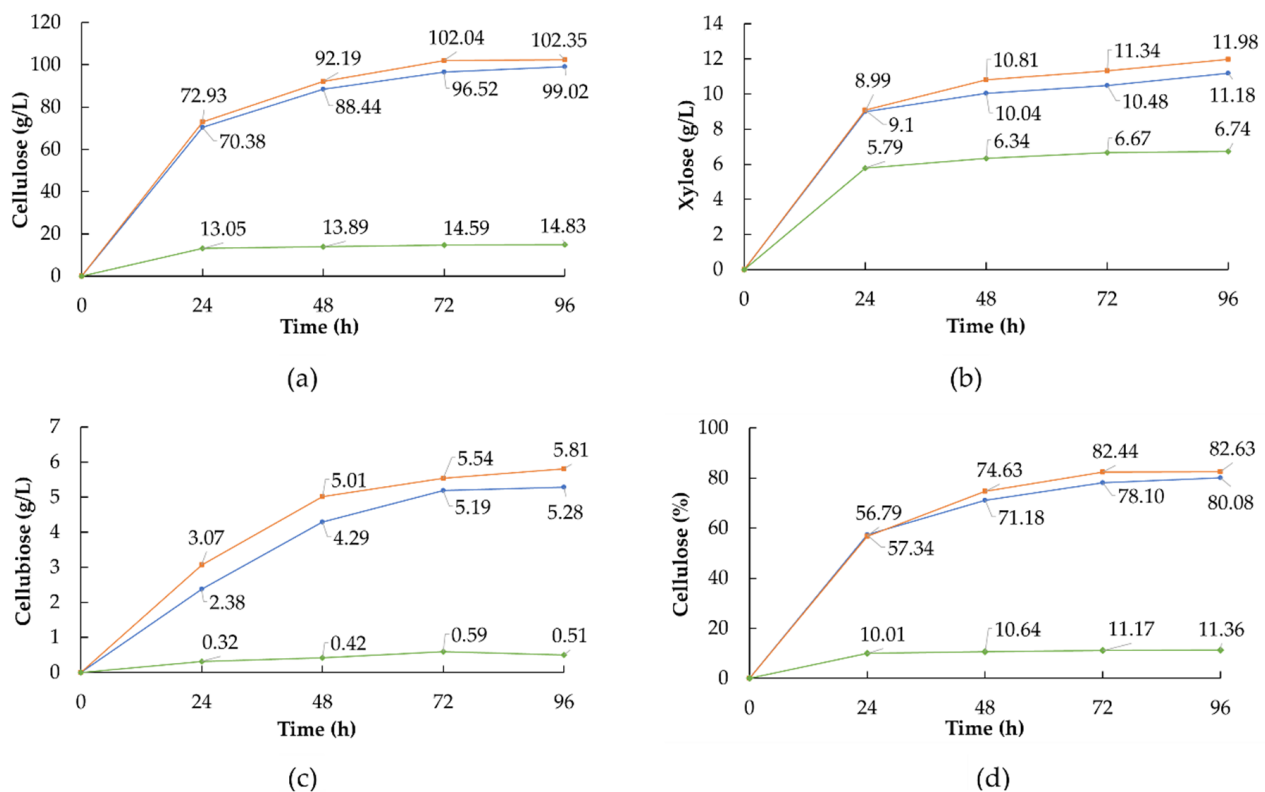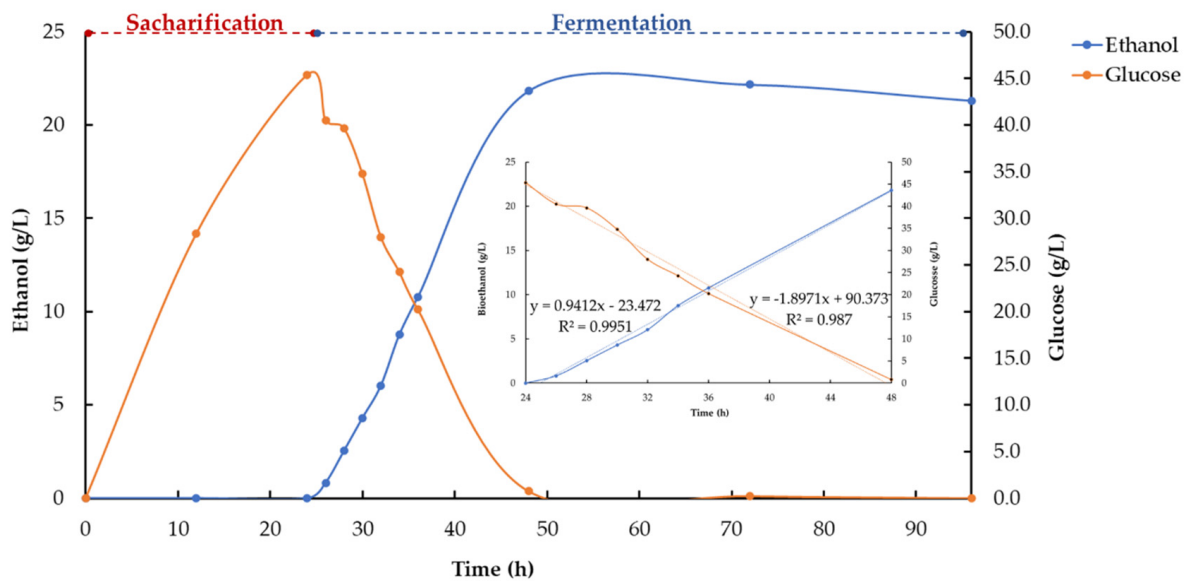
Figure 4. Saccharification process kinetics. (**a**) Glucose concentration (g/L); (**b**) xylose concentration (g/L); (**c**) cellobiose concentration (g/L); (**d**) saccharification yield (%). Data are mean values of triplicate experiments. ◆ Correspond at 0 FPU, ● at 10 FPU, and ■ at 15 FPU.

### 3.4. Pre-Simultaneous Saccharification and Fermentation (PSSF)

PSSF consisted of the SSB prehydrolyzing at an optimal temperature for the enzymes (high enzymatic activity). After 24 h, the reactor was cooled to an ideal temperature for fermentation (yeast). In addition, PSSF allows the use of a high solids load since it reduces the suspension's initial viscosity before fermentation starts [55]. PSSF process kinetics is shown in Figure 5, in which an increase in glucose concentration can be observed in the first 24 h due to the action of the enzymes on the substrate (saccharification). From 24 to 48 h, a linear decrease of 97.48% glucose was observed, with a consumption rate of 1.90 g/L/h, related to the establishment and growth of the yeast in the medium (fermentation). From 48 to 96 h, minimum glucose levels were detected. In the box of Figure 5, the fermentation process kinetics presented the typical phases of yeast growth, as it has been reported for the fermentation of sorghum juice fermented with *Saccharomyces cerevisiae* PE-2 [56]. Thus, in the first 24 h of fermentation, it had a linear behavior, with a bioethanol production rate of 0.94 g/L/h, which is equivalent to 98.42% of the maximum obtained in the process at 48 h (22.17 g/L) and which remains constant until the end. This behavior and yield were like those reported for other sorghum varieties [37,39]. Although after 48 h of treatment, the glucose concentration was below 0.78 g/L, the maintenance of the culture and the production of bioethanol can be explained by the presence of residual xylose and XOS that are preserved in the bagasse.

Figure 5. Process of pre-saccharification kinetics and simultaneous fermentation (PSSF).

On the other hand, the bioethanol conversion rate at 24 h of fermentation was 2.47%, with a yield in the process of 57.32% (Figure 6). Therefore, the fermentation process can be stopped after 24 h and thus reduce costs by saving resources and energy. In this sense, a wide range of bioethanol yields has been reported using different production technologies. For example, Thanapimmetha et al. [39], using different methods of simultaneous saccharification and fermentation (SSF), obtained yields of 22.30 and 28.30 g/L in SSB. Su et al. [40], applying a pretreatment with NaOH in SSB, reported a bioethanol yield of 50.80 ± 3.20 g/L from an initial 111.50 g/L of glucose. Matsakas and Christakopoulos. [57], with the liquefaction of pretreated SSB, obtained 41.43 g/L and a productivity of 1.88 g/L/h. Furthermore, they increased the concentration of bioethanol by adding additional enzymes at the start of saccharification. On the other hand, Tinôco et al. [58] reached 17.83 g/L of bioethanol at 42 °C in 24 h, using SSB pretreated with base acid and saccharification at 50 °C for 72 h. Thus, among the factors that can influence bioethanol yield are the type of reactor, load and enzymes blend in saccharification, initial availability of fermentable sugars, solids load, temperature, time, type of yeast, and raw material.
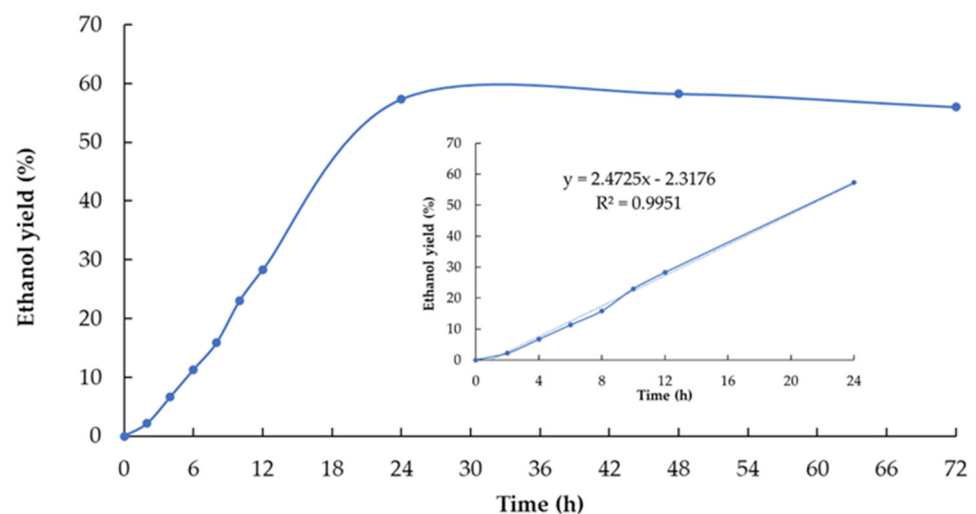
Figure 6. Bioethanol yield.

3.5. Energy Balance in the Bioethanol Production Process

Table 5 shows the net energy balance of the process. The total energy consumption in the bioethanol production process was 229.03 MJ, equivalent to 2.46 MJ/g of SSB processed, of which 79.14% was by concept of electricity (181.26 MJ), with PSSF being the stage of the process with the highest demand (154.58 MJ, at equivalent to 1.67 MJ/g). This consumption was associated with the technology used, where electricity is the principal source for the operation of the facilities and mechanized equipment used. Accordingly, an alternative that can reduce electricity consumption is to make the most of the work capacity of these means. For example, increasing the solids load in the autohydrolysis and enzymatic pretreatment [27], in addition to the unit processes integration, is recommended to improve performance, reduce reaction time, and make better use of the resources and materials generated [8,54,57].

Table 5. Energy balance in the bioethanol production process.

FE	Processes				E_{inp} (MJ)	E_{out} (MJ)
	GD (MJ)	HP (MJ)	AH (MJ)	PSSF (MJ)		
Electricity	0.79	29.73	25.35	125.39	181.26	-
Human labor	3.01	1.75	5.88	29.1	39.74	-
Chemicals	0.00	0.00	6.54	0.00	6.54	-
Enzymes	0.00	0.00	0.00	0.04	0.04	-
Yeasts	0.00	0.00	0.00	0.05	0.05	-
Water	0.00	0.47	0.93	0.0025	1.40	-
Total	3.80	31.95	38.71	154.58	229.03	2.52
Energy consumed per unit of processed biomass * (MJ/g)						
Electricity	0.01	0.32	0.27	1.35	1.94	-
Human labor	0.03	0.02	0.06	0.31	0.43	-
Chemicals	0.00	0.00	0.07	0.00	0.07	-
Enzymes	0.00	0.00	0.00	0.0004	0.0004	-
Yeasts	0.00	0.00	0.00	0.0005	0.0005	-
Water	0.00	0.01	0.01	0.00	0.02	-
E_{inp}	0.04	0.34	0.42	1.67	2.46	-
E_{out}	-	-	-	-	-	0.03

FE = forms of energy; GD = grinding; HP = hydrothermal pretreatment; AH = acid hydrolysis; EH = enzymatic hydrolysis; PSSF = pre-saccharification simultaneous and fermentation; E_{inp} = energy input; E_{out} = energy output; * Processed biomass weight = 93.2 g.

On the other hand, the difference between the energy obtained (E_{out} = 0.03 MJ/g) from bioethanol and the energy consumed in obtaining it (2.46 MJ/g) was notable. This result affects the process's energy efficiency. It can be explained by the volume of SSB processed per energy unit, the yield of bioethanol obtained (Section 3.4), and its calorific value (Table 2), among other factors. These may vary depending on the technology used and the source of origin of the raw material (renewable and non-renewable) [35,59]. In this sense, energy efficiency can be increased by integrating the lignin and other products derived from the process of obtaining bioethanol (cogeneration) [19,22], in addition to integrating biochemical, thermochemical, physical, and catalytic conversion to produce a wide range of biobased products [54], reusing the water and soluble products [60], as well as the carbon dioxide (CO_2) released during fermentation as a carbon source for other crops [61]. In general, this information can be used to compare different production scenarios in energetic terms and select the best operating conditions that contribute to increasing efficiency [21].

4. Conclusions

The chemical composition of SSB allows it to be used as a feedstock to produce second-generation bioethanol from a hydrothermal pretreatment process followed by simultaneous pre-saccharification and fermentation. Furthermore, the increase in the severe conditions of the pretreatment resulted in a higher release of fermentable sugars and energy consumption. In the process of pre-saccharification and simultaneous fermentation, fermentation time can be carried out by 24 h, with a bioethanol yield of 98.42%. Moreover, the energy input was higher concerning the energy output of the bioethanol production process, which resulted in lower energy efficiency.

References

1. López-Sandin, I.; Gutiérrez-Soto, G.; Gutiérrez-Díez, A.; Medina-Herrera, N.; Gutiérrez-Castorena, E.; Zavala-García, F. Evaluation of the use of energy in the production of sweet sorghum (*Sorghum bicolor* (L.) Moench) under different production systems. *Energies* **2019**, *12*, 1713. [CrossRef]
2. Ruiz, H.A.; Thomsen, M.H.; Trajano, H.L. *Hydothermal Processing in Biorefineries*, 1st ed.; Springer: Cham, Switzerland, 2017; pp. v–viii. [CrossRef]
3. Kumar, M.N.; Ravikumar, R.; Thenmozhi, S.; Kumar, M.R.; Shankar, M.K. Choice of pretreatment technology for sustainable production of bioethanol from lignocellulosic biomass: Bottle necks and recommendations. *Waste Biomass Valoris.* **2019**, *10*, 1693–1709. [CrossRef]
4. Ruiz, H.A.; Rodriguez, R.M.; Fernandes, B.D.; Vicente, A.; Teixeira, A. Hydrothermal processing, as an alternative for upgrading agriculture residues and marine biomass according to the biorefinery concept: A review. *Renew. Sustain. Energy Rev.* **2013**, *21*, 35–51. [CrossRef]
5. Rosero-Chasoy, G.; Rodríguez-Jasso, R.M.; Aguilar, C.N.; Buitrón, G.; Chairez, I.; Ruiz, H.A. Hydrothermal kinetic modeling for microalgae biomass under subcritical condition cultivated in a close bubble tubular photobioreactor. *Fuel* **2023**, *334*, 126585. [CrossRef]
6. Demichelis, F.; Laghezza, M.; Chiappero, M.; Fiore, S. Technical, economic and environmental assessement of bioethanol biorefinery from waste biomass. *J. Clean. Prod.* **2020**, *277*, 124111. [CrossRef]

7. Morales-Contreras, B.E.; Flórez-Fernández, N.; Torres, M.D.; Domínguez, H.; Rodríguez-Jasso, R.M.; Ruiz, H.A. Hydrothermal systems to obtain high value-added compounds from macroalgae for bioeconomy and biorefineries. *Bioresour. Technol.* **2022**, *343*, 126017. [CrossRef] [PubMed]

8. Reshmy, R.; Paulose, T.A.P.; Philip, E.; Thomas, D.; Madhavan, A.; Sirohi, R.; Binod, P.; Awasthi, M.K.; Pandey, A.; Sindhu, R. Updates on high value products from cellulosic biorefinery. *Fuel* **2022**, *308*, 122056. [CrossRef]

9. Srivastava, N.; Rawat, R.; Singh Oberoi, H.; Ramteke, P.W. A review on fuel ethanol production from lignocellulosic biomass. *Int. J. Green Energy* **2015**, *12*, 949–960. [CrossRef]

10. Partida-Sedas, G.; Montes-García, N.; Carvajal-Zarrabal, O.; López-Zamora, L.; Gómez-Rodríguez, J.; Aguilar-Uscanga, M.G. Optimization of hydrolysis process to obtain fermentable sugars from sweet sorghum bagasse using a Box–Behnken design. *Sugar Tech.* **2017**, *19*, 317–325. [CrossRef]

11. Velmurugan, B.; Narra, M.; Rudakiya, D.M.; Madamwar, D. Sweet sorghum: A potential resource for bioenergy production. In *Refining Biomass Residues for Sustainable Energy and Bioproducts: Technology, Advances, Life Cycle Assessment and Economics*, 1st ed.; Kumar, R.P., Edgard Gnansounou, E., Raman, J.K., Baskar, G., Eds.; Academic Press: Cambridge, MA, USA, 2020; Volume 1, pp. 215–242. [CrossRef]

12. Nazli, R.I. Evaluation of different sweet sorghum cultivars for bioethanol yield potential and bagasse combustion characteristics in a semiarid Mediterranean environment. *Biomass Bioenergy* **2020**, *139*, 105624. [CrossRef]

13. Xiao, M.Z.; Sun, Q.; Hong, S.; Chen, W.J.; Pang, B.; Du, Z.Y.; Wen-Bin, Y.; Zhuohua, S.; Yuan, T.Q. Sweet sorghum for phytoremediation and bioethanol production. *J. Leather Sci. Eng.* **2021**, *3*, 1–23. [CrossRef]

14. Ximenes, E.; Farinas, C.S.; Kim, Y.; Ladisch, M.R. Hydrothermal pretreatment of lignocellulosic biomass for bioethanol production. In *Hydrothermal Processing in Biorefineries*, 1st ed.; Ruiz, A.H., Mette, M.H., Trajano, H.L., Eds.; Springer Nature: Cham, Switzerland, 2017; Volume 1, pp. 181–205. [CrossRef]

15. Ruiz, H.A.; Galbe, M.; Garrote, G.; Ramirez-Gutierrez, D.M.; Ximenes, E.; Sun, S.N.; Lachos-Perez, D.; Rodríguez-Jasso, R.M.; Run-Cang, S.; Yang, B.; et al. Severity factor kinetic model as a strategic parameter of hydrothermal processing (steam explosion and liquid hot water) for biomass fractionation under biorefinery concept. *Bioresour. Technol.* **2021**, *342*, 125961. [CrossRef]

16. Cybulska, I.; Thomsen, M.H. Bioethanol production from pretreated solids using hydrothermal processing. In *Hydrothermal Processing in Biorefineries*; Springer: Cham, Switzerland, 2017; pp. 237–252. [CrossRef]

17. Huang, C.; Jiang, X.; Shen, X.; Hu, J.; Tang, W.; Wu, X.; Ragauskas, A.; Jameel, H.; Meng, X.; Yong, Q. Lignin-enzyme interaction: A roadblock for efficient enzymatic hydrolysis of lignocellulosics. *Renew. Sustain. Energy Rev.* **2022**, *154*, 111822. [CrossRef]

18. Rezania, S.; Oryani, B.; Cho, J.; Talaiekhozani, A.; Sabbagh, F.; Hashemi, B.; Rupani, P.F.; Mohammadi, A.A. Different pretreatment technologies of lignocellulosic biomass for bioethanol production: An overview. *Energy* **2020**, *199*, 117457. [CrossRef]

19. Ruiz, H.A.; Conrad, M.; Sun, S.N.; Sanchez, A.; Rocha, G.J.; Romaní, A.; Castro, E.; Torres, A.; Rodríguez-Jasso, R.M.; Andrade, L.P.; et al. Engineering aspects of hydrothermal pretreatment: From batch to continuous operation, scale-up and pilot reactor under biorefinery concept. *Bioresour. Technol.* **2020**, *299*, 122685. [CrossRef]

20. Aristizábal-Marulanda, V.; Solarte-Toro, J.C.; Alzate, C.A.C. Study of biorefineries based on experimental data: Production of bioethanol, biogas, syngas, and electricity using coffee-cut stems as raw material. *Environ. Sci. Pollut. Res.* **2021**, *28*, 24590–24604. [CrossRef]

21. Elyasi, S.N.; Rafiee, S.; Mohtasebi, S.S.; Tsapekos, P.; Angelidaki, I.; Liu, H.; Khoshnevisan, B. An integer superstructure model to find a sustainable biorefinery platform for valorizing household waste to bioenergy, microbial protein, and biochemicals. *J. Clean. Prod.* **2021**, *278*, 123986. [CrossRef]

22. Islam, M.K.; Thaemngoen, A.; Lau, C.Y.; Guan, J.; Yeung, C.S.; Chaiprapat, S.; Leu, S.Y. Staged organosolv pretreatment to increase net energy and reactive lignin yield in whole oil palm tree biorefinery. *Bioresour. Technol.* **2021**, *326*, 124766. [CrossRef]

23. Nitsos, C.K.; Matis, K.A.; Triantafyllidis, K.S. Optimization of hydrothermal pretreatment of lignocellulosic biomass in the bioethanol production process. *ChemSusChem* **2012**, *6*, 110–122. [CrossRef]

24. Sluiter, A.; Hames, B.; Ruiz, R.; Scarlata, C.; Sluiter, J.; Templeton, D.; Crocker, D.L.A.P. Determination of Ash in Biomass. *Lab. Anal. Proced. (LAP)* **2005**, *NREL/TP-510-42622*, 1–8.

25. Sluiter, A.; Hames, B.; Ruiz, R.; Scarlata, C.; Sluiter, J.; Templeton, D.; Crocker, D.L.A.P. Determination of structural carbohydrates and lignin in biomass. *Lab. Anal. Proced. (LAP)* **2005**, *NREL/TP-510-42618*, 1–17.

26. Zhu, J.Y.; Pan, X.; Zalesny, R.S. Pretreatment of woody biomass for biofuel production: Energy efficiency, technologies, and recalcitrance. *Appl. Microbiol. Biotechnol* **2010**, *87*, 847–857. [CrossRef] [PubMed]

27. Shiva; Rodríguez-Jasso, R.M.; Rosero-Chasoy, G.; López-Sandin, I.; Morais, A.R.C.; Ruiz, H.A. Enzymatic hydrolysis, kinetic modeling of hemicellulose fraction, and energy efficiency of autohydrolysis pretreatment using agave bagasse. *BioEnergy Res.* **2022**, 1–13. [CrossRef]

28. Adney, B.; Nrel, J.B. Measurement of Cellulase Activities. *Meas. Cell. Act. Lab. Anal. Proced. LAP* **1996**, *NREL/TP-510-42628*, 1–11.

29. Aparicio, E.; Rodríguez-Jasso, R.M.; Pinales-Márquez, C.D.; Loredo-Treviño, A.; Robledo-Olivo, A.; Aguilar, C.N.; Kostas, E.T.; Ruiz, H.A. High-pressure technology for *Sargassum* spp. biomass pretreatment and fractionation in the third generation of bioethanol production. *Bioresour. Technol.* **2021**, *329*, 124935. [CrossRef]

30. Qing, Q. The Effects of Surfactant Pretreatment and Xylooligomers on Enzymatic Hydrolysis of Cellulose and Pretreated Biomass. Ph.D. Dissertation, University of California Riverside, Riverside, CA, USA, August 2010. Available online: https://escholarship.org/uc/item/5hc293kb (accessed on 20 April 2022).

31. Dowe, N.; McMillan, J. SSF Experimental Protocols: Lignocellulosic Biomass Hydrolysis and Fermentation. *Natl. Renew. Energy Lab. NREL Anal. Proced.* **2001**, *NREL/TP-510-42630*, 1–19. Available online: https://www.nrel.gov/docs/gen/fy08/42630.pdf (accessed on 10 March 2022).

32. Mayer, F.D.; Brondani, M.; Carrillo, M.C.V.; Hoffmann, R.; Lora, E.E.S. Revisiting energy efficiency, renewability, and sustainability indicators in biofuels life cycle: Analysis and standardization proposal. *J. Clean. Prod.* **2020**, *252*, 119850. [CrossRef]

33. Saga, K.; Imou, K.; Yokoyama, S.; Minowa, T. Net energy analysis of bioethanol production system from high-yield rice plant in Japan. *Appl. Energy* **2010**, *87*, 2164–2168. [CrossRef]

34. Bernesson, S. Life Cycle Assessment of Rapeseed Oil, Rape Methyl Ester and Ethanol as Fuels—A Comparison between Large-and Small Scale Production. U.S. Department of Energy Office of Scientific and Technical Information, Studsvik Library, SE-611 82 Nykoeping, Sweden. 2004; p. 267. Available online: https://www.osti.gov/etdeweb/servlets/purl/20567425 (accessed on 20 April 2022).

35. Bentsen, N.S.; Felby, C.; Ipsen, K.H. Energy Balance of 2nd Generation Bioethanol Production in Denmark. *DONG Energy* **2006**, 43. Available online: https://www.researchgate.net/profile/Niclas-Bentsen/publication/237534730_ENERGY_BALANCE_OF_2nd_GENERATION_BIOETHANOL_PRODUCTION_IN_DENMARK/links/00b495320d4dba1cf5000000/ENERGY-BALANCE-OF-2nd-GENERATION-BIOETHANOL-PRODUCTION-IN-DENMARK.pdf (accessed on 20 April 2022).

36. Zou, L.; Wan, Y.; Zhang, S.; Luo, J.; Li, Y.Y.; Liu, J. Valorization of food waste to multiple bio-energies based on enzymatic pretreatment: A critical review and blueprint for the future. *J. Clean. Prod.* **2020**, *277*, 124091. [CrossRef]

37. Heredia-Olea, E.; Pérez-Carrillo, E.; Montoya-Chiw, M.; Serna-Saldívar, S.O. Effects of extrusion pretreatment parameters on sweet sorghum bagasse enzymatic hydrolysis and its subsequent conversion into bioethanol. *BioMed Res. Int.* **2015**, *2015*, 1–10. [CrossRef]

38. Wen, H.; Chen, H.; Cai, D.; Gong, P.; Zhang, T.; Wu, Z.; Tan, T. Integrated in situ gas stripping–salting-out process for high-titer acetone–butanol–ethanol production from sweet sorghum bagasse. *Biotechnol. Biofuels* **2018**, *11*, 1–12. [CrossRef]

39. Thanapimmetha, A.; Saisriyoot, M.; Khomlaem, C.; Chisti, Y.; Srinophakun, P. A comparison of methods of ethanol production from sweet sorghum bagasse. *Biochem. Eng. J.* **2019**, *151*, 107352. [CrossRef]

40. Su, C.; Qi, L.; Cai, D.; Chen, B.; Chen, H.; Zhang, C.; Si, Z.; Wang, Z.; Li, G.; Qin, P. Integrated ethanol fermentation and acetone-butanol-ethanol fermentation using sweet sorghum bagasse. *Renew. Energy* **2020**, *162*, 1125–1131. [CrossRef]

41. De Almeida, L.G.F.; da Costa Parrella, R.A.; Simeone, M.L.F.; de Oliveira Ribeiro, P.C.; dos Santos, A.S.; da Costa, A.S.V.; Gonçalves Guimarães, A.G.; Schaffert, R.E. Composition and growth of sorghum biomass genotypes for ethanol production. *Biomass Bioenergy* **2019**, *122*, 343–348. [CrossRef]

42. Cesarino, I.; Araújo, P.; Domingues Júnior, A.P.; Mazzafera, P. An overview of lignin metabolism and its effect on biomass recalcitrance. *Braz. J. Bot.* **2012**, *35*, 303–311. [CrossRef]

43. Pino, M.S.; Rodríguez-Jasso, R.M.; Michelin, M.; Ruiz, H.A. Enhancement and modeling of enzymatic hydrolysis on cellulose from agave bagasse hydrothermally pretreated in a horizontal bioreactor. *Carbohydr. Polym.* **2019**, *211*, 349–359. [CrossRef]

44. Yu, J.; Zhang, X.; Tan, T. Ethanol production by solid state fermentation of sweet sorghum using thermotolerant yeast strain. *Fuel Process. Technol.* **2008**, *89*, 1056–1059. [CrossRef]

45. Ewanick, S.; Bura, R. Hydrothermal pretreatment of lignocellulosic biomass. In *Bioalcohol Production*, 1st ed.; Keith Waldron, K., Ed.; Woodhead Publishing Series in Energy; Woodhead Publishing: Amsterdam, The Netherlands, 2010; Volume 1, pp. 3–23. [CrossRef]

46. Singh, R.; Liu, H.; Shanklin, J.; Singh, V. Hydrothermal pretreatment for valorization of genetically engineered bioenergy crop for lipid and cellulosic sugar recovery. *Bioresour. Technol.* **2021**, *341*, 125817. [CrossRef]

47. Geffert, A.; Geffertova, J.; Dudiak, M. Direct method of measuring the pH value of wood. *Forests* **2019**, *10*, 852. [CrossRef]

48. Lin, R.; Deng, C.; Ding, L.; Bose, A.; Murphy, J.D. Improving gaseous biofuel production from seaweed *Saccharina latissima*: The effect of hydrothermal pretreatment on energy efficiency. *Energy Convers. Manag.* **2019**, *196*, 1385–1394. [CrossRef]

49. Bedzo, O.K.; Dreyer, C.B.; van Rensburg, E.; Görgens, J.F. Optimisation of pretreatment catalyst, enzyme cocktail and solid loading for improved ethanol production from sweet sorghum bagasse. *BioEnergy Res.* **2022**, *15*, 1083–1095. [CrossRef]

50. De Freitas, C.; Carmona, E.; Brienzo, M. Xylooligosaccharides production process from lignocellulosic biomass and bioactive effects. *Bioact. Carbohydr. Diet. Fibre* **2019**, *18*, 100184. [CrossRef]

51. Huang, C.; Yu, Y.; Li, Z.; Yan, B.; Pei, W.; Wu, H. The preparation technology and application of xylo-oligosaccharide as prebiotics in different fields: A review. *Front. Nutr.* **2022**, *9*, 996811. [CrossRef] [PubMed]

52. Pal, P.; Kumar, S.; Devi, M.M.; Saravanamurugan, S. Oxidation of 5-hydroxymethylfurfural to 5-formyl furan-2-carboxylic acid by non-precious transition metal oxide-based catalyst. *J. Supercrit. Fluids* **2020**, *160*, 104812. [CrossRef]

53. Pinales-Márquez, C.D.; Rodríguez-Jasso, R.M.; Araújo, R.G.; Loredo-Trevino, A.; Nabarlatz, D.; Gullón, B.; Ruiz, H.A. Circular bioeconomy and integrated biorefinery in the production of xylooligosaccharides from lignocellulosic biomass: A review. *Ind. Crops Prod.* **2021**, *162*, 113274. [CrossRef]

54. Velvizhi, G.; Balakumar, K.; Shetti, N.P.; Ahmad, E.; Pant, K.K.; Aminabhavi, T.M. Integrated Biorefinery Processes for Conversion of Lignocellulosic Biomass to Value Added Materials: Paving a Path Towards Circular Economy. *Bioresour. Technol.* **2021**, *343*, 126151. [CrossRef]

55. De Barros, E.M.; Carvalho, V.M.; Rodrigues, T.H.S.; Rocha, M.V.P.; Gonçalves, L.R.B. Comparison of strategies for the simultaneous saccharification and fermentation of cashew apple bagasse using a thermotolerant Kluyveromyces marxianus to enhance cellulosic ethanol production. *Chem. Eng. J.* **2017**, *307*, 939–947. [CrossRef]

56. López-Sandin, I.; Zavala-García, F.; Levin, L.; Ruiz, H.A.; Hernández-Luna, C.E.; Gutiérrez-Soto, G. Evaluation of bioethanol production from sweet sorghum variety roger under different tillage and fertilizer treatments. *BioEnergy Res.* **2021**, *14*, 1058–1069. [CrossRef]

57. Matsakas, L.; Christakopoulos, P. Fermentation of liquefacted hydrothermally pretreated sweet sorghum bagasse to ethanol at high-solids content. *Bioresour. Technol.* **2013**, *127*, 202–208. [CrossRef]

58. Tinôco, D.; Genier, H.L.A.; da Silveira, W.B. Technology valuation of cellulosic ethanol production by *Kluyveromyces marxianus* CCT 7735 from sweet sorghum bagasse at elevated temperatures. *Renew. Energy* **2021**, *173*, 188–196. [CrossRef]

59. Mofijur, M.; Ong, H.C.; Jan, B.M.; Kusumo, F.; Sebayang, A.H.; Husin, H.; Silitonga, A.S.; Indra Mahlia, T.M.; Rahman, S.A. Production process and optimization of solid bioethanol from empty fruit bunches of palm oil using response surface methodology. *Process* **2019**, *7*, 715. [CrossRef]

60. Couto, E.; Calijuri, M.L.; Assemany, P. Biomass production in high-rate ponds and hydrothermal liquefaction: Wastewater treatment and bioenergy integration. *Sci. Total Environ.* **2020**, *724*, 138104. [CrossRef]

61. Souza, S.P.; Gopal, A.R.; Seabra, J.E. Life cycle assessment of biofuels from an integrated Brazilian algae-sugarcane biorefinery. *Energy* **2015**, *81*, 373–381. [CrossRef]